SUPPORTING INFORMATION

$Ce(OH)_2Cl$ and Lanthanide-Substituted Variants as Precursors to Redox- Active CeO_2 Materials

Alexander J.A. Dunn,[†] James Annis,[†] Janet M. Fisher,[‡] David Thompsett[‡] and Richard I. Walton,[†*]

[†]*Department of Chemistry, University of Warwick, Coventry, CV4 7AL, UK. *Email r.i.walton@warwick.ac.uk*

[‡]*Johnson Matthey Technology Centre, Sonning Common, Reading, RG4 9NH, UK*

S1: Further analysis of $Ce_{1-x}Ln_x(OH)_2Cl$ materials

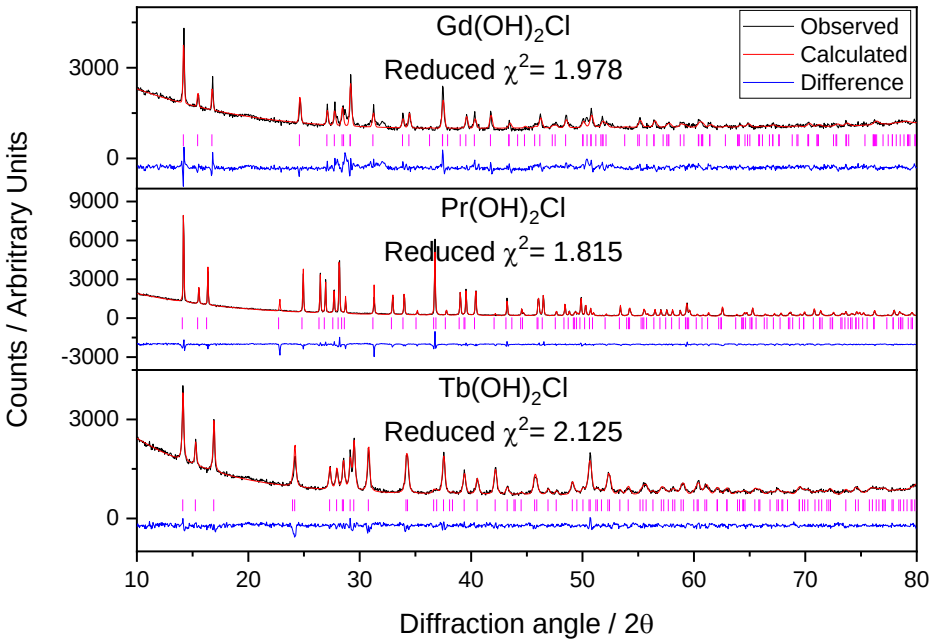

Figure S1.1 Le Bail fits to Powder XRD data (λ = 1.5405 Å) of $Tb(OH)_2Cl$, $Pr(OH)_2Cl$ and $Gd(OH)_2Cl$.

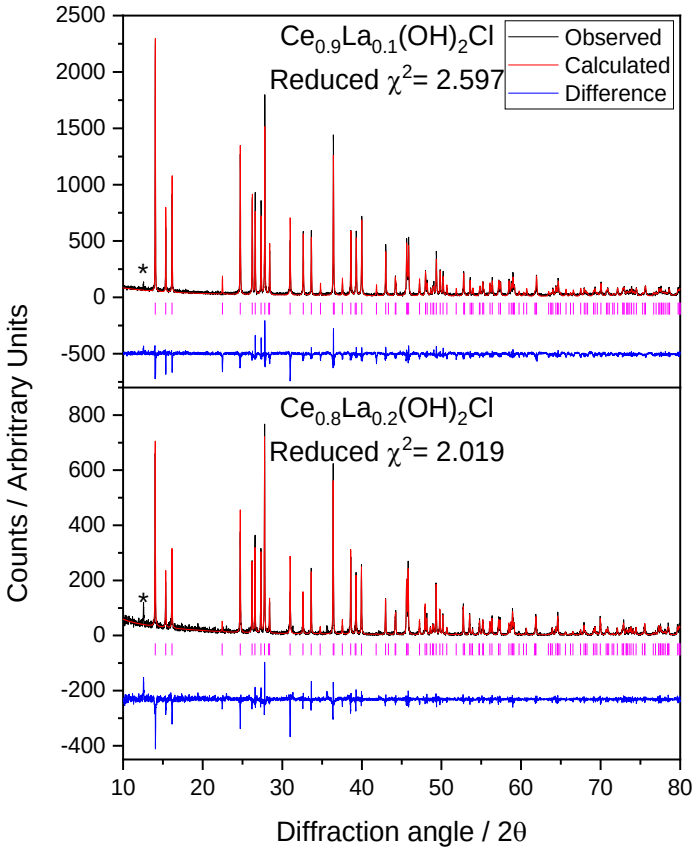

Figure S1.2: Le Bail fits to Powder XRD data (λ = 1.5405 Å) of $Ce_{1-x}La_x(OH)_2Cl$ ($0.1 \leq x \leq 0.2$). (contamination on XRD slit).*

Table S1.1: Results of Le Bail fitting to powder XRD data of $Ce_{1-x}La_x(OH)_2Cl$ ($0.1 \leq x \leq 0.2$).

Sample	*a* (Å)	*b* (Å)	*c* (Å)	β (Å)	Volume (Å^3)
$Ce_{0.9}La_{0.1}(OH)_2Cl$	6.2925 (1)	6.8802 (1)	3.95446 (7)	113.542 (1)	156.952 (3)
$Ce_{0.8}La_{0.2}(OH)_2Cl$	6.29485 (11)	6.88596 (11)	3.95854 (6)	113.585 (1)	157.254 (3)

Table S1.2: Measured values of x from SEM EDXA elemental analysis of $Ce_{1-x}La_x(OH)_2Cl$.

Sample	Atomic %		STDEV
	Ce	La	
$Ce_{0.9}La_{0.1}(OH)_2Cl$	90	10	0.4
$Ce_{0.8}La_{0.2}(OH)_2Cl$	78.6	21.4	0.7

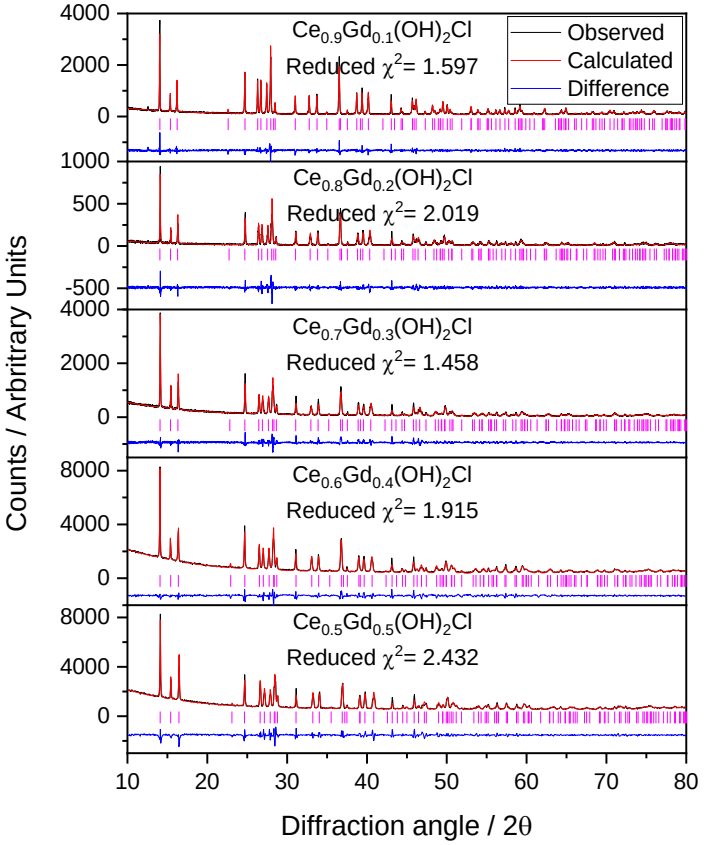

Figure S1.3: Le Bail fits to Powder XRD data (λ = 1.5405 Å) of $Ce_{1-x}Gd_x(OH)_2Cl$ ($0.1 \leq x \leq 0.5$).

Table S1.3: Results of Le Bail fitting to powder XRD data of $Ce_{1-x}Gd_x(OH)_2Cl$ ($0.1 \leq x \leq 1$).

Sample	*a* (Å)	*b* (Å)	*c* (Å)	*β* (Å)	Volume (Å^3)
$Ce_{0.9}Gd_{0.1}(OH)_2Cl$	6.27420 (14)	6.86038 (14)	3.93040 (8)	113.317 (1)	155.361 (7)
$Ce_{0.8}Gd_{0.2}(OH)_2Cl$	6.2599 (2)	6.8466 (2)	3.91150 (16)	113.139 (2)	154.157 (7)
$Ce_{0.7}Gd_{0.3}(OH)_2Cl$	6.2469 (2)	6.8328 (2)	3.89483 (14)	112.963 (2)	153.073 (7)
$Ce_{0.6}Gd_{0.4}(OH)_2Cl$	6.2330 (4)	6.8182 (7)	3.8769 (3)	112.776 (4)	151.914 (2)
$Ce_{0.5}Gd_{0.5}(OH)_2Cl$	6.2194 (4)	6.8013 (4)	3.8501 (4)	112.494 (5)	150.468 (15)

Table S1.4 Measured values of x from SEM EDXA elemental analysis of $Ce_{1-x}Gd_x(OH)_2Cl$.

Sample	Atomic %		STDEV
	Ce	Gd	
$Ce_{0.9}Gd_{0.1}(OH)_2Cl$	89.9	10.1	1.2
$Ce_{0.8}Gd_{0.2}(OH)_2Cl$	78.7	21.3	3.4
$Ce_{0.7}Gd_{0.3}(OH)_2Cl$	73.6	26.4	2.8
$Ce_{0.6}Gd_{0.4}(OH)_2Cl$	59.6	40.4	3.2
$Ce_{0.5}Gd_{0.5}(OH)_2Cl$	53.7	46.3	1.9

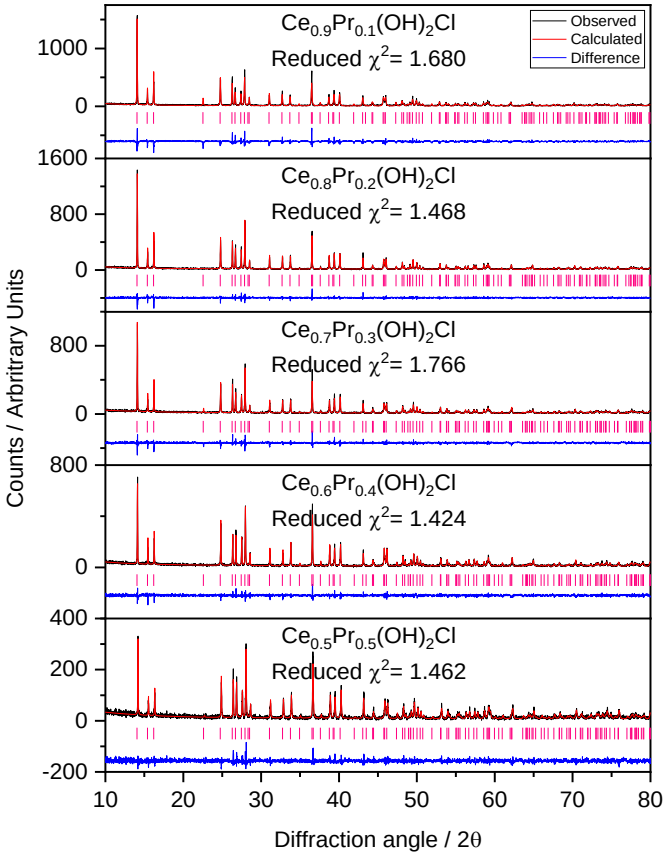

Figure S1.4: Le Bail fits to Powder XRD data (λ = 1.5405 Å) of $Ce_{1-x}Pr_x(OH)_2Cl$ ($0.1 \leq x \leq 0.5$).

Table S1.5: Results of Le Bail fitting to powder XRD data of $Ce_{1-x}Pr_x(OH)_2Cl$ ($0.1 \leq x \leq 1$).

Sample	*a* (Å)	*b* (Å)	*c* (Å)	*β* (Å)	Volume (Å^3)
$Ce_{0.9}Pr_{0.1}(OH)_2Cl$	6.2843 (2)	6.87381 (18)	3.94754 (13)	113.502 (2)	156.378 (6)
$Ce_{0.8}Pr_{0.2}(OH)_2Cl$	6.28042 (11)	6.8716 (1)	3.94320 (7)	113.491 (1)	156.070 (3)
$Ce_{0.7}Pr_{0.3}(OH)_2Cl$	6.27653 (15)	6.86907 (13)	3.93933 (9)	113.482 (1)	155.774 (4)
$Ce_{0.6}Pr_{0.4}(OH)_2Cl$	6.27272 (14)	6.86629 (13)	3.93577 (8)	113.460 (1)	155.503 (4)
$Ce_{0.5}Pr_{0.5}(OH)_2Cl$	6.2712 (2)	6.8673 (2)	3.93342 (13)	113.457 (2)	155.397 (6)
$Pr(OH)_2Cl$	6.24778 (17)	6.85337 (17)	3.9132 (1)	113.416 (2)	153.756 (5)

Table S1.6: Measured values of x from SEM EDX elemental analysis of $Ce_{1-x}Pr_x(OH)_2Cl$.

Sample	Atomic %		STDEV
	Ce	Pr	
$Ce_{0.9}Pr_{0.1}(OH)_2Cl$	89.4	10.6	0.3
$Ce_{0.8}Pr_{0.2}(OH)_2Cl$	79.7	20.3	0.6
$Ce_{0.7}Pr_{0.3}(OH)_2Cl$	69.3	30.7	0.6
$Ce_{0.6}Pr_{0.4}(OH)_2Cl$	58.7	41.3	0.4
$Ce_{0.5}Pr_{0.5}(OH)_2Cl$	51.5	48.5	0.5

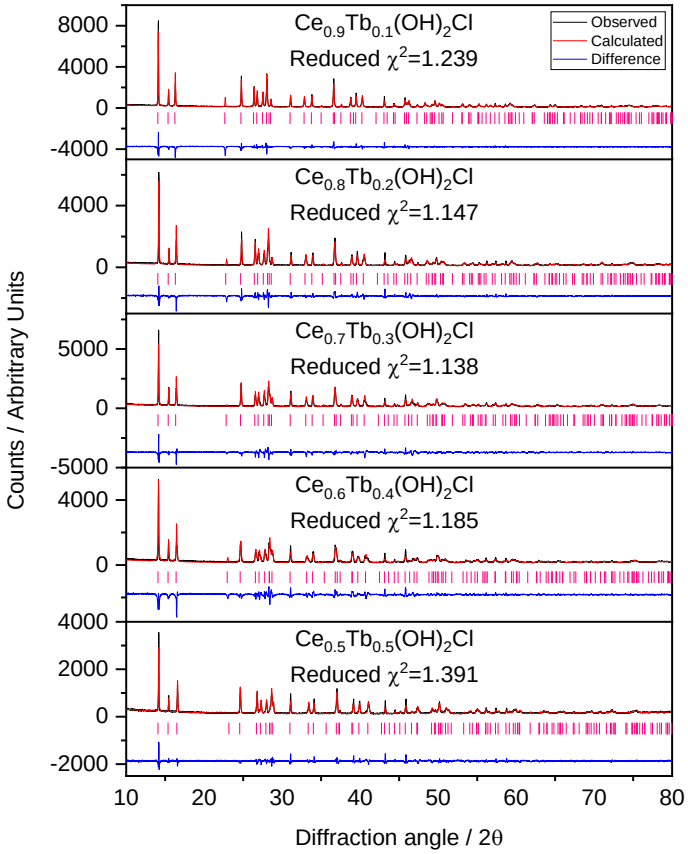

Figure S1.5: Le Bail fits to Powder XRD data (λ = 1.5405 Å) of $Ce_{1-x}Tb_x(OH)_2Cl$ ($0.1 \leq x \leq 0.5$).

Table S1.7: Results of Le Bail fitting to powder XRD data of $Ce_{1-x}Tb_x(OH)_2Cl$ ($0.1 \leq x \leq 1$).

Sample	*a* (Å)	*b* (Å)	*c* (Å)	*β* (Å)	Volume (Å^3)
$Ce_{0.9}Tb_{0.1}(OH)_2Cl$	6.2726 (3)	6.8570 (3)	3.92680 (14)	113.244 (2)	155.187 (12)
$Ce_{0.8}Tb_{0.2}(OH)_2Cl$	6.2581 (3)	6.8395 (2)	3.90568 (16)	112.976 (2)	153.910 (7)
$Ce_{0.7}Tb_{0.3}(OH)_2Cl$	6.2493 (3)	6.8259 (4)	3.89468 (17)	112.811 (2)	153.142 (15)
$Ce_{0.6}Tb_{0.4}(OH)_2Cl$	6.2401 (6)	6.8100 (8)	3.8716 (4)	112.526 (4)	151.97 (3)
$Ce_{0.5}Tb_{0.5}(OH)_2Cl$	6.2232 (2)	6.7851 (3)	3.83724 (16)	112.072 (2)	150.153 (12)
$Tb(OH)_2Cl$	6.1790 (4)	6.6749 (6)	3.7102 (3)	109.956 (6)	143.835 (14)

Table S1.8: Measured values of x from SEM EDXA elemental analysis of $Ce_{1-x}Tb_x(OH)_2Cl$.

Sample	Atomic %		STDEV
	Ce	Tb	
$Ce_{0.9}Tb_{0.1}(OH)_2Cl$	88.6	11.4	1.5
$Ce_{0.8}Tb_{0.2}(OH)_2Cl$	78.3	21.7	2.0
$Ce_{0.7}Tb_{0.3}(OH)_2Cl$	69.5	30.5	1.8
$Ce_{0.6}Tb_{0.4}(OH)_2Cl$	58.5	41.5	2.1
$Ce_{0.5}Tb_{0.5}(OH)_2Cl$	51.8	48.2	1.4

S2: Further SEM of $Ce_{1-x}Ln_x(OH)_2Cl$ materials and their oxide products

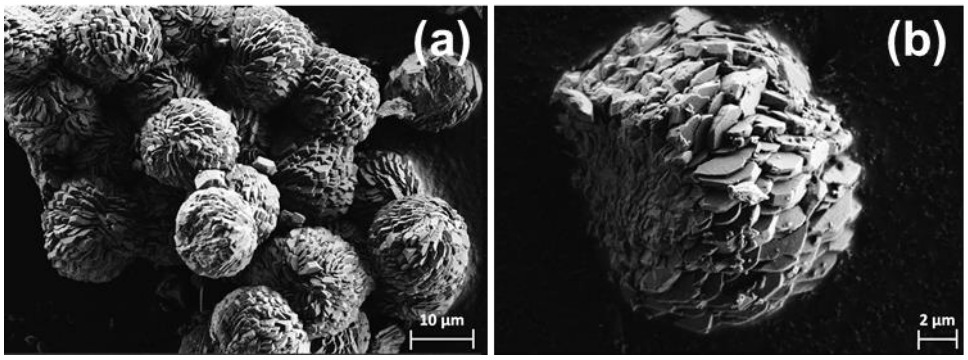

Figure S2.1: SEM images of $Ce_{0.9}Ln_{0.1}(OH)_2Cl$ as-made (a) and after heating at 700 °C (b)

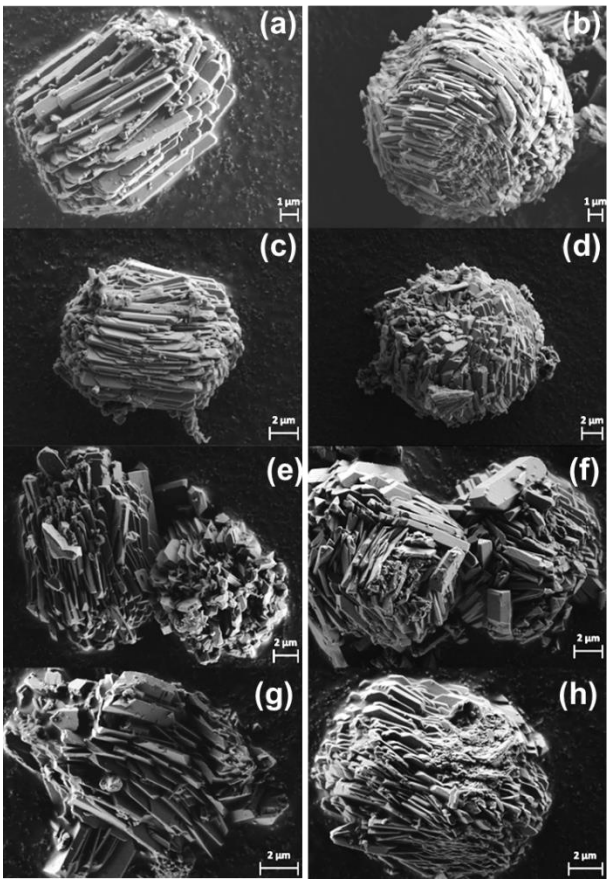

Figure S2.2: SEM images of $Ce_{1-x}Pr_x(OH)_2Cl$ as-made (left) and after heating at 700 °C (right) heating for (a) and (b) x = 0.1, (c) and (d) x = 0.2, (e) and (f) x = 0.3, (g) and (h) x = 0.4.

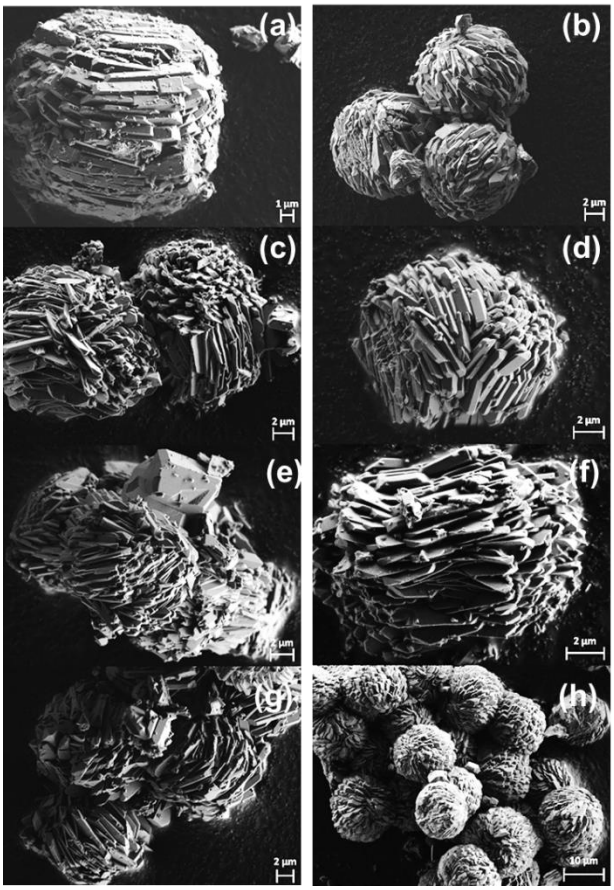

Figure S2.3: SEM images of $Ce_{1-x}Gd_x(OH)_2Cl$ as-made (left) and after heating at 700 °C (right) heating for (a) and (b) x = 0.1, (c) and (d) x = 0.2, (e) and (f) x = 0.3, (g) and (h) x = 0.4.

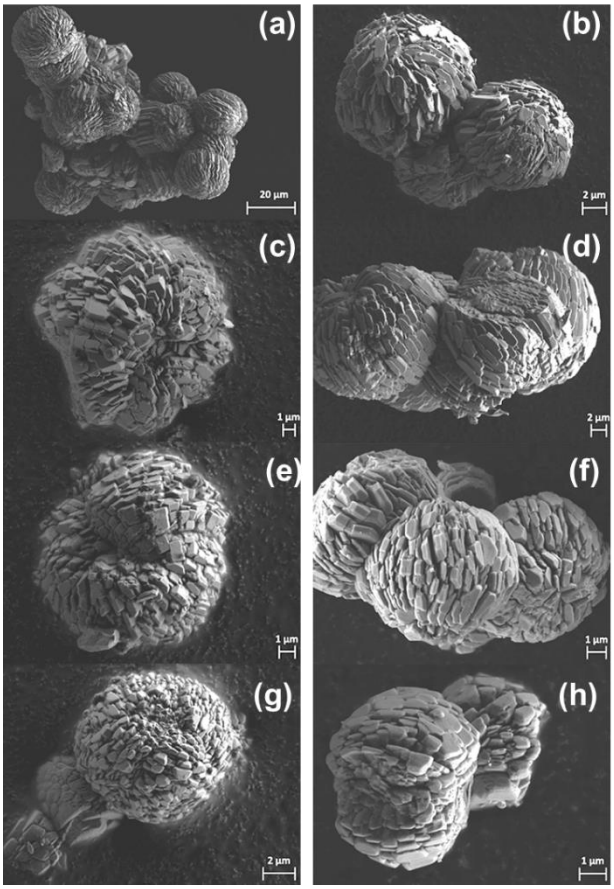

Figure S2.4: SEM images of $Ce_{1-x}Tb_x(OH)_2Cl$ as-made (left) and after heating at 700 °C (right) heating for (a) and (b) x = 0.1, (c) and (d) x = 0.2, (e) and (f) x = 0.3, (g) and (h) x = 0.4.

S3: Powder XRD analysis of $Ce_{1-x}Ln_xO_{2-\delta}$ oxides

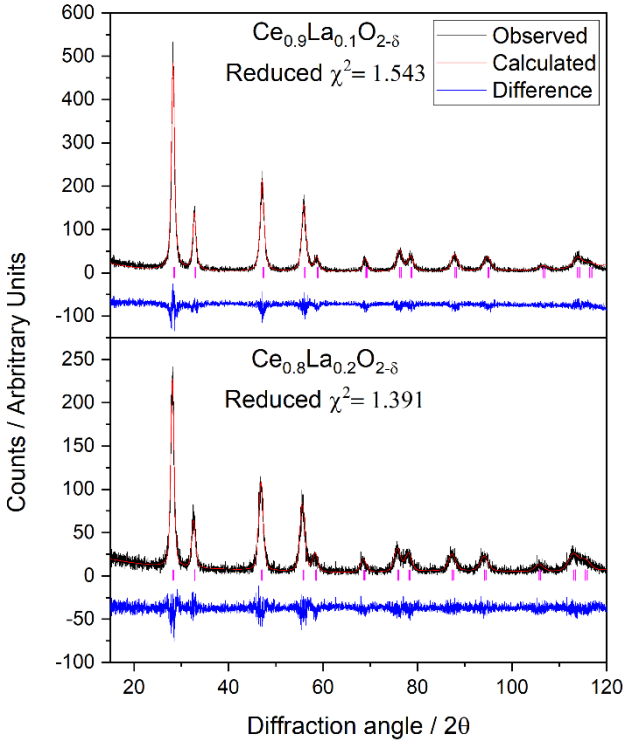

Figure S3.1: Profile fits of $Ce_{1-x}La_xO_{2-\delta}$ oxides

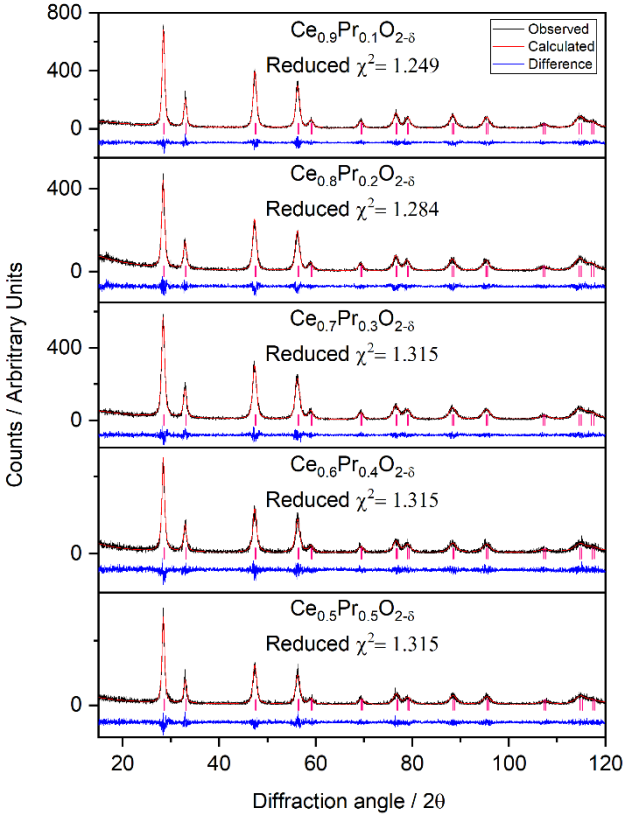

Figure S3.2: Profile fits of $Ce_{1-x}Pr_xO_{2-\delta}$ oxides

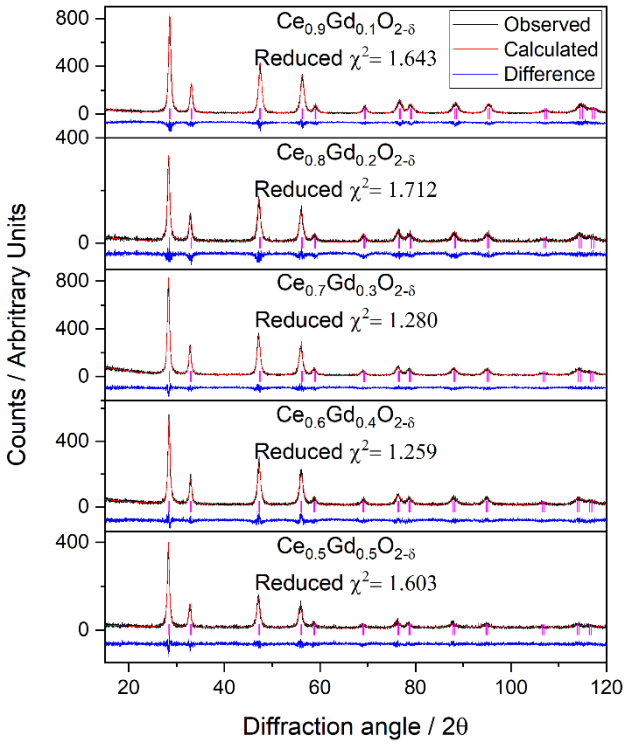

Figure S3.3: Profile fits of $Ce_{1-x}Gd_xO_{2-\delta}$ oxides

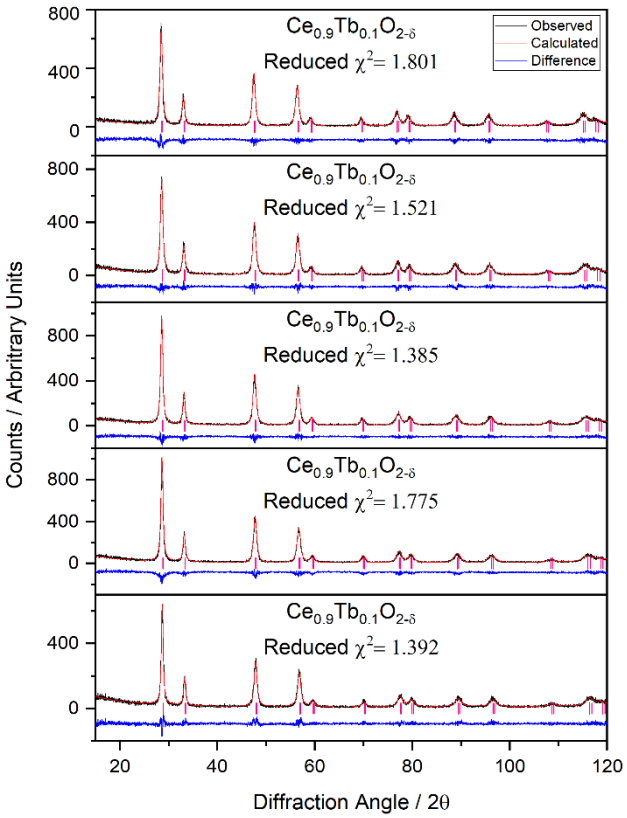

Figure S3.4: Profile fits of $Ce_{1-x}Tb_xO_{2-\delta}$ oxides

Williamson-Hall analysis was performed using Equation S1:

$$B\cos\theta = C\varepsilon\sin\theta + \frac{K\lambda}{L}$$

Symbol	Definition
B	Line broadening (FWHM)
θ	Bragg angle
Cε	Strain component
K	Shape factor
λ	X-ray wavelength (Å)
L	Crystallite size (Å)

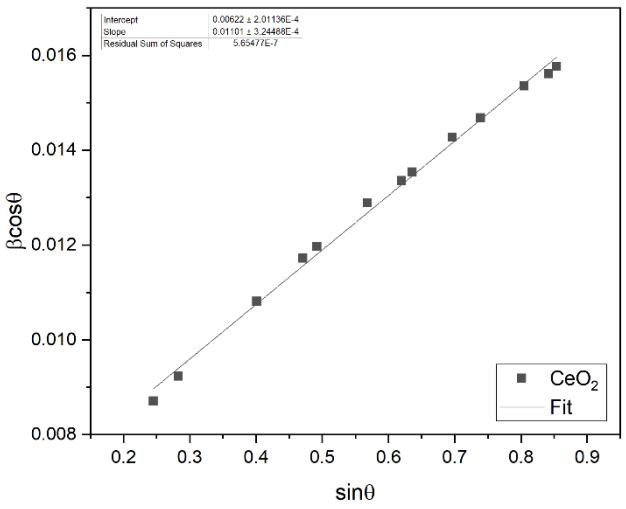

Figure S3.5: Williamson-Hall plot for CeO_2

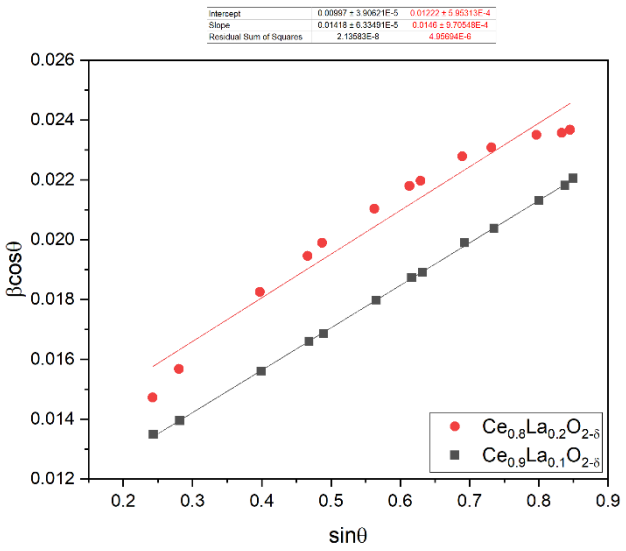

Figure S3.6: Williamson-Hall plots for $Ce_{1-x}La_xO_{2-\delta}$ oxides

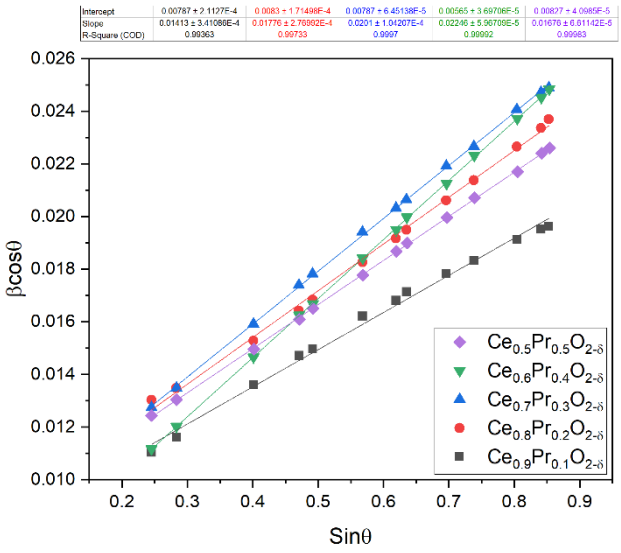

Figure S3.7: Williamson-Hall plots for $Ce_{1-x}Pr_xO_{2-\delta}$ oxides

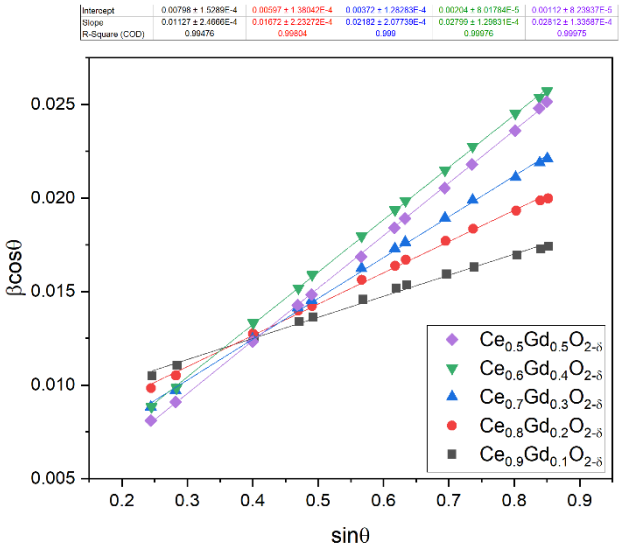

Figure S3.8: Williamson-Hall plots for $Ce_{1-x}Gd_xO_{2-\delta}$ oxides

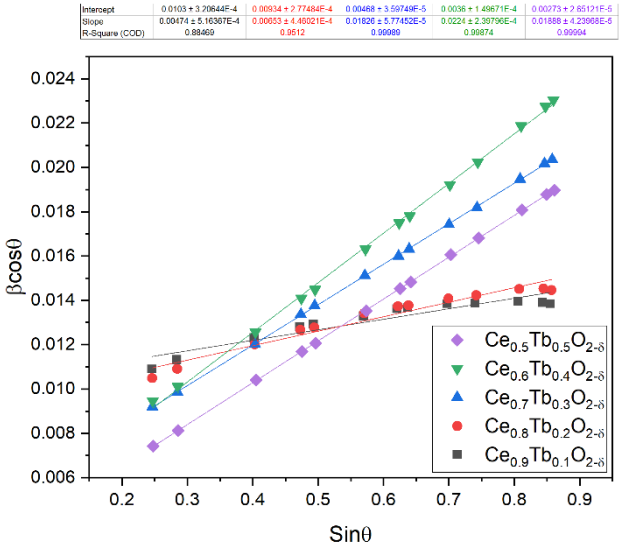

Figure S3.9: Williamson-Hall plots for $Ce_{1-x}Tb_xO_{2-\delta}$ oxides

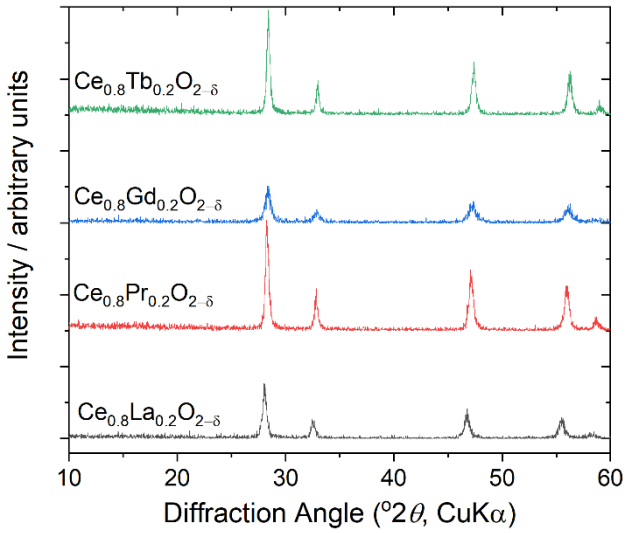

Figure S3.10: XRD patterns after two TPR cycles for $Ce_{1-x}Ln_xO_{2-\delta}$ oxides

S4: Synthesis of $CeCO_3(OH)$

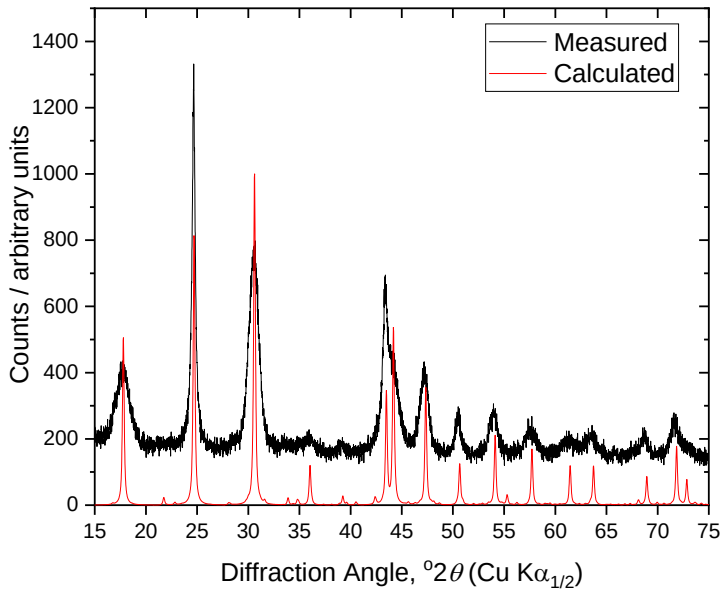

Figure S4.1: Powder XRD of $CeCO_3(OH)$ prepared using $Ce(NO_3)_3 \cdot 6H_2O$ in PEG M_n = 200 . The calculated patterns is from the published structure of Michiba *et al.*[1]

1. Michiba, K.; Miyawaki, R.; Minakawa, T.; Terada, Y.; Nakai, I.; Matsubara, S., Crystal structure of hydroxylbastnäsite-(Ce) from Kamihouri, Miyazaki Prefecture, Japan. *Journal of Mineralogical and Petrological Sciences* **2013,** *108*, 326-334.